EUROPEAN JOURNAL OF PURE AND APPLIED MATHEMATICS
2026, Vol. 19, Issue 2, Article Number 7159
ISSN 1307-5543 – ejpam.com
Published by New York Business Global

Nonlinear Dynamics of Specific Physical Waves and Bifurcation in Beta-Fractional (2+1)-Dimensional Kadomtsev–Petviashvili Equation

Ahmed Ramady[1,2], Mohammed S. Ghayad[3], M. Y. Hamada[4], Hamdy M. Ahmed[5], M. Elsaid Ramadan[6], Soliman Alkhatib[7], Karim K. Ahmed[4,*]

[1] *GRC Department, The Applied College, King Abdulaziz University, Jeddah, 21589, Saudi Arabia*
[2] *Department of Mathematics and computer science, Faculty of Science, Beni-Suef University, Beni-Suef, Egypt*
[3] *Department of Physics and Engineering Mathematics, Faculty of Engineering, Ain Shams University, Cairo, Egypt*
[4] *Department of Mathematics, Faculty of Engineering, German International University (GIU), New Administrative Capital, Cairo, Egypt*
[5] *Department of Mathematics and Engineering Physics, Higher Institute of Engineering, El-Shorouk Academy, El-Shorouk city, Cairo, Egypt*
[6] *Department of Mathematics, Faculty of Science, Islamic University of Madinah, Medina, Saudi Arabia*
[7] *College of Engineering and Technology (CET), American University in the Emirates (AUE), Dubai intel Academic City, P.O. Box 503000, Dubai, United Arab Emirates*

Abstract. This paper derives novel exact elliptic solutions for the (2+1)-dimensional Kadomtsev-Petviashvili equation and the Shallow Water Waves equation with beta-fractional derivative using the improved modified extended (IME) tanh method. The originality of the paper resides in the fact that the IME method was generalized for the fractional dispersive equations for the first time, resulting in a wide variety of new wave patterns, namely the bright and dark solitons, singular solitons, Jacobi elliptic waves, periodic, singular periodic, and hyperbolic solutions. The applicability of the obtained results is justified by the fact that these wave patterns are capable of characterizing the nonlocal wave processes occurring in shallow water and plasma-like media. Additionally, a bifurcation and stability analysis was also carried out, and the effects of the most significant parameters of the system on wave phenomena and transfer processes have been clarified. The obtained results are verified and illustrated using detailed 2D, 3D, and polar plots along with the phase portrait analysis.

2020 Mathematics Subject Classifications: 35C08, 35Q51, 35E99, 37K40
Key Words and Phrases: Soliton solutions, kadomtsev–Petviashvili model, fractional derivatives, improved modified extended tanh function approach, bifurcation analysis.

*Corresponding Author.
DOI: https://doi.org/10.29020/nybg.ejpam.v19i2.7159

Email addresses: karim.kamal.502@gmail.com (Karim K. Ahmed)

 Copyright: © 2026 The Author(s). (CC BY-NC 4.0)

1. Introduction

Nonlinear evolution equations (NLEEs) are crucial tools for modeling complex systems in a variety of domains, such as biology, engineering, physics, and finance. The capacity to uncover the underlying principles that underlie nonlinear phenomena makes the analytical determination of their exact solutions a vital and ever-evolving area of research [1–4].

Solitons are unique self-sustaining wave packets that don't undergo much deformation over long distances. They are ideal for reliable information conveyance since they retain their shape and amplitude while propagating [5, 6]. Mathematicians and physicists have been fascinated by nonlinear wave phenomena for millennia because they are essential to comprehending the complex dynamics of various physical systems. The behavior of waves in plasmas and condensed matter, as well as the propagation of light in optical fibers, are examples of complicated processes that may be described using nonlinear wave equations.

Recent studies have shown the applicability and potential of the methods for the exploration of nonlinear dispersive waves. New exact solutions for dispersive solitary wave solutions have been found for dynamical soliton equations using the methods developed and investigated by Bilal et al., [7]. Likewise, various exact optical soliton solutions have also been found for the (2+1)-dimensional conformable fractional Schrödinger equation using the methods developed and investigated by Bilal and Ahmad [8]. Several issues concerning the significance of fractional equations have also emerged from the study pursued by the authors of the paper being investigated. M. Ahmad [9] developed and investigated the properties of the concepts and the theories developed for exploring multi-lump solutions, soliton collisions, and interactions with stability analysis. Results concerning three-dimensional shallow wave equations have also emerged for the study pursued by Shafqat-Ur-Rehman et al., [10] for solitary wave solutions.

To study soliton solutions, several analytical techniques have been developed, such as the complex Hirota bilinear approach [11], the Bäcklund and Darboux transformations [12, 13], and the inverse scattering transform [14]. The balance between dispersion and nonlinearity is the main determinant of soliton interaction behavior. Solitons may interchange energy when they have the same frequency. This phenomenon is called soliton resonance, and it can result in complex interaction patterns that emphasize the system's nonlinearity. Solitons often create stable bound states as a result of their interactions, which are necessary for optical fiber communications to transmit data over long distances with little signal degradation [15–17].

The recent achievements in developing effective solution methods for solving fractional- and higher-dimensional nonlinear systems fall into a prominent class of interest in the current work. Indeed, necessary and efficient solution methods have been found to tackle local fractional nonlinear systems [18], while simplified analytical solution approaches have managed to treat complex wave dynamics within the framework of a class of higher-dimensional nonlinear systems like the (3+1)-dimensional wave equation [19]. Also, the study of complex wave structures like the soliton molecule and interaction has found application within a class of integrable nonlinear systems [20, 21]. In recent years, a wide range of advanced analytical techniques have been developed and applied to derive exact solutions of NLEEs with high precision. Among these are the Kudryashov method [22], the Sardar sub-equation approach [23], and the Jacobi elliptic function (JEF) expansion algorithm [24], all of which have demonstrated significant efficiency in handling complex nonlinear structures. Similarly, the Simple Equations method based on composite functions [25] and the IME tanh-function technique [26, 27] have proven highly effective in obtaining diverse solution forms. Furthermore, other robust strategies have been greatly employed to construct solitons, periodic, and some rational solutions, including the ϕ^6-model expansion scheme [28], the modified extended direct algebraic method (mEDAM) [29, 30], and Lie symmetry analysis [31]. These symbolic computational tools play a critical role across multiple scientific and engineering disciplines, providing a systematic framework for analyzing, decomposing, and solving intricate nonlinear models, particularly those arising in mathematical physics, fluid dynamics, plasma theory, and nonlinear optics.

Combining integral and differential components, integral-partial differential equations (IPDEs) are essential for modeling a range of real-world events where memory effects and cumulative dynamics play a significant role [32, 33]. Integro-differential equations provide a robust framework for modeling systems characterized by hereditary effects, where present dynamics are influenced by past states. Their applicability spans diverse fields: in physics, they describe viscoelastic materials whose stress relies on deformation history; in ecology, they model population growth dependent on historical levels; and in engineering, they govern electrical circuits with memory-based components like capacitors. This hybrid nature, combining instantaneous change with cumulative past influence, renders them indispensable for analyzing systems with distributed delays or memory.

Numerous writers looked at their dynamical behaviors because of their significance. In [34–36], a novel structured (2+1)-dimensional nonlinear model known as the Kadomtsev–Petviashvili equation is examined. One way to write this equation is:

$$(\mathcal{T}_t + 6\mathcal{T}\mathcal{T}_x + \mathcal{T}_{xxx})_x + 3\mathcal{T}_{xx}\left(\int_{-\infty}^{x} \mathcal{T}_y\, dx\right) + 6\mathcal{T}_x\mathcal{T}_y + \mathcal{T}_{xxxy} + \delta\mathcal{T}_{xy} + 3\mathcal{T}\mathcal{T}_{xy} + \mathcal{T}_{yt} - \sigma\mathcal{T}_{yy} = 0. \tag{1}$$

To correctly describe nonlocal and memory effects in optical wave propagation, the fractional counterpart of the traditional IPDEs was adopted. In many optical systems, including photonic crystals and extremely dispersive fiber optics, wave dynamics show long-range interactions and anomalous dispersion that can be completely described with integer-order derivatives. By adding a history-dependent impact on soliton behavior, the fractional derivative added to the classical IPDEs generalizes the standard model. For this reason, we change the previous equation to be:

$$\left(D_t^{\beta}\mathcal{T} + 6\mathcal{T}\mathcal{T}_x + \mathcal{T}_{xxx}\right)_x + 3\mathcal{T}_{xx}\left(\int_{-\infty}^{x} \mathcal{T}_y\, dx\right) + 6\mathcal{T}_x\mathcal{T}_y + \mathcal{T}_{xxxy} + \delta\mathcal{T}_{xy} + 3\mathcal{T}\mathcal{T}_{xy} + D_t^{\beta}\mathcal{T}_y - \sigma\mathcal{T}_{yy} = 0, \tag{2}$$

when δ and σ are real constants not equal to zero, the analytic function to be found is represented by the equation $\mathcal{T} = \mathcal{T}(x, y, t)$. The term D^{β} represents the beta-fractional derivative of order $0 < \beta \leq 1$.

The idea of fractional derivatives is examined in the study, as it provides a strong foundation for describing nonlocal effects in actual systems. Applications for fractional calculus are diverse and include modeling the behavior of molecules and materials [37, 38], wave propagation through incompressible fluids and shallow water [39], circuit theory, and biology [40, 41]. The motivation of this study arises from the growing importance of fractional-order models in describing complex nonlinear phenomena with greater accuracy compared to classical integer-order approaches. In particular, the shallow water wave and $(2+1)$-dimensional Kadomtsev–Petviashvili equations with beta-fractional derivatives provide a more realistic framework for capturing memory and hereditary effects that naturally occur in wave propagation in fluids, plasmas, and other dispersive media. Despite the extensive literature on integer-order forms of these models, exact solutions under fractional derivatives remain limited. Therefore, our work aims to enrich the set of available analytical solutions by employing the IME tanh-function approach. This approach not only yields diverse classes of nonlinear structures such as solitons, periodic waves, and Jacobi elliptic solutions, but also facilitates a detailed analysis of their stability and bifurcation behavior. Such analysis is crucial for understanding the robustness, persistence, and potential applications of the obtained solutions in realistic physical systems.

The motivation of this work is to extend the classical (2+1)-dimensional Kadomtsev–Petviashvili equation within a fractional framework while preserving mathematical locality and analytical solvability. The beta-fractional derivative is a local fractional operator that generalizes the classical time derivative through a fractional order without introducing nonlocal integral memory terms. This property makes it particularly suitable for nonlinear wave models where exact analytical treatment, stability analysis, and bifurcation theory are required. Although the beta-fractional derivative modifies wave propagation characteristics through the fractional order parameter β, exact solution structures and their qualitative dynamics remain largely unexplored for beta-fractional KP-type equations. Moreover, existing studies rarely combine exact solution construction with stability and bifurcation analysis in a unified setting. In addition, this study employs the IME tanh-function method to derive novel soliton wave solutions that have not been previously documented. These solutions encompass bright, dark, singular, periodic, singular periodic, Weierstrass elliptic doubly periodic, Jacobi elliptic, hyperbolic, and exponential types. The influence of the beta-fractional derivative on these solutions is systematically examined. Furthermore, stability and bifurcation analyses are conducted to provide a comprehensive understanding of the dynamical behavior of the obtained solutions.

The structure of the manuscript is as follows: Section 1 introduces the proposed model with its physical interpretation and theory. Section 2 formulates the mathematical requirements of the IME tanh-function method along with an elaborate explanation of its construction, validity, and advantages in solving different kinds of nonlinear models, in addition to some mathematical preliminaries about the beta-fractional derivative. Section 3 is dedicated to the formulation of the mathematical model and basic equations of the proposed model, reflecting the application of the IME tanh-function technique to the process of the solution. Section 4 is dedicated to a full graphical analysis, where 2D, 3D, contour, and polar plots are employed for the description of the dynamical behaviors of the obtained soliton wave structures under varying parameter conditions. Section 5 illustrates how the suggested model is mapped into a planar system, simplifying the study of its principal properties. Section 6 is dedicated to stability and bifurcation analyses, providing insight into the nonlinear dynamics of the system and its key switching points. Section 7 introduces the physical interpretation and model validation of this study. Section 8 concludes the principal findings, highlights the novel contributions and applications of the research, and offers suggestions for future research directions.

2. Mathematical preliminaries

In this section, we provide basic mathematical preliminaries for the fractional derivative used in this paper, and also the main steps of the algorithm used.

2.1. Beta-fractional derivative

The beta-fractional derivative is a local fractional operator. It modifies the classical derivative through a time-scaling factor $(t + \frac{1}{\Gamma(\beta)})^{1-\beta}$, preserving the basic structure of integer-order calculus (linearity, product rule, chain rule) without involving integral kernels or historical memory integrals. The beta-fractional derivative describes weak or short-range memory effects arising from time-dependent scaling, microstructural heterogeneity, or effective damping mechanisms, while maintaining local behavior. The fractional order modifies the instantaneous response rather than accumulating historical effects.

Definition 1. *Let $\mathcal{T}$ be a function such that [41, 42]*

$$\mathcal{T} : [0, \infty) \to \mathbb{R}.$$

Next, a function $\mathcal{T}$ has a beta derivative that is defined as

$$D_t^{\beta}\mathcal{T}(t) = \lim_{\epsilon \to 0} \frac{\mathcal{T}\left(t + \epsilon\left(t + \frac{1}{\Gamma(\beta)}\right)^{1-\beta}\right) - \mathcal{T}(t)}{\epsilon},$$

for all $t \geq 0,\ \beta \in (0, 1]$. If the limit exists, $\mathcal{T}$ is said to be β-differentiable.

The fractional derivative D^{β} used in this study satisfies several important properties:

- Linearity:

$$D^{\beta}\left(a\mathcal{T}(t) + b\mathcal{S}(t)\right) = aD^{\beta}\mathcal{T}(t) + bD^{\beta}\mathcal{S}(t), \quad \forall a, b \in \mathbb{R},$$

- Product rule:

$$D^{\beta}\left(\mathcal{T}(t)\mathcal{S}(t)\right) = \mathcal{T}(t)D^{\beta}\mathcal{S}(t) + \mathcal{S}(t)D^{\beta}\mathcal{T}(t),$$

- Quotient rule:

$$D^{\beta}\left(\frac{\mathcal{T}(t)}{\mathcal{S}(t)}\right)=\frac{\mathcal{S}(t)D^{\beta}\mathcal{T}(t)-\mathcal{T}(t)D^{\beta}\mathcal{S}(t)}{(\mathcal{S}(t))^{2}},$$

- Fundamental definition:

$$D^{\beta}\mathcal{T}(t)=\left(t+\frac{1}{\Gamma(\beta)}\right)^{1-\beta}\frac{d\mathcal{T}(t)}{dt},$$

- Fractional chain rule:

$$D^{\beta}\left(\mathcal{T}(\mathcal{S}(t))\right)=\mathcal{S}'(t)^{\beta}D^{\beta}\mathcal{T}(\mathcal{S}(t)).$$

2.2. The improved modified extended tanh function approach in brief

The IME tanh-function method improves solution accuracy and structural variety by providing an effective analytical tool for building exact soliton and wave solutions to a wide class of nonlinear evolution equations. The IME tanh function technique is particularly useful for researching complicated physical processes in domains like fluid dynamics, plasma physics, and optical fiber systems since it improves on conventional tanh-based techniques and enables more compact and generalized forms of solutions.
The general processes of the IME tanh-function technique are shown here, and they will be used in the next part. Upon beginning to examine the following nonlinear partial differential equation (NPDE) displayed below [27, 28]:

$$\mathcal{E}\left(\mathcal{Q},\mathcal{Q}_x,\mathcal{Q}_y,D_t^{\beta}\mathcal{Q},\mathcal{Q}_{xx},D_t^{\beta}\mathcal{Q}_x,...\right)=0,\tag{3}$$

where $\mathcal{E}$ is a polynomial function of $\mathcal{Q}(x,y,t)$ in addition to some partial derivatives of $\mathcal{Q}$ with respect to the two-dimensional space of the studied dynamical system (x,y) and time t.

Step (I): Consider the following transformation [43, 44]:

$$\mathcal{Q}(x,y,t)=\mathcal{P}(\zeta),\quad \zeta=x+ky-\vartheta\frac{\left(t+\frac{1}{\Gamma(\beta)}\right)^{\beta}}{\beta},\tag{4}$$

where k and ϑ are some real constants, and $\mathcal{P}$ represents the wave profile of the solution to be evaluated.

By inserting Eq. (4) into the governing equation (3) and performing appropriate rearrangements, the original partial differential equation is reduced to the following nonlinear ordinary differential equation (NLODE):

$$\mathcal{Z}\big(\mathcal{P},\mathcal{P}',\mathcal{P}'',\mathcal{P}''',\dots\big)=0.\tag{5}$$

Step (II): To construct the exact solution of Eq. (5) via the implemented method, the solution $\mathcal{P}(\zeta)$ is assumed to take the truncated series form:

$$\mathcal{P}(\zeta)=\sum_{i=0}^{\mathbb{N}}\mathfrak{A}_i\mathcal{W}^{i}(\zeta)+\sum_{i=1}^{\mathbb{N}}\mathfrak{B}_i\mathcal{W}^{-i}(\zeta),\tag{6}$$

where the constants $\mathfrak{A}_0, \mathfrak{A}_1, \ldots, \mathfrak{A}_{\mathbb{N}}$ and $\mathfrak{B}_1, \ldots, \mathfrak{B}_{\mathbb{N}}$ are real parameters to be determined. At least one of the leading coefficients $\mathfrak{A}_{\mathbb{N}}$ or $\mathfrak{B}_{\mathbb{N}}$ must be non-zero to ensure a non-trivial solution.

Step (III): The homogeneous balance principle is implemented on Eq. (5) to determine the value of the balancing constant $\mathbb{N}$ by equating the highest-order nonlinear term with the highest-order derivative term. In addition, $\mathcal{W}(\zeta)$ is assumed to satisfy the following auxiliary ordinary differential equation:

$$\mathcal{W}'(\zeta) = \Omega\sqrt{\lambda_0 + \lambda_1\mathcal{W}(\zeta) + \lambda_2\mathcal{W}^2(\zeta) + \lambda_3\mathcal{W}^3(\zeta) + \lambda_4\mathcal{W}^4(\zeta)}, \tag{7}$$

where $\Omega = \pm 1$ and λ_m $(0 \leq m \leq 4)$ considered as real-valued constants. By selecting appropriate combinations of the parameters $\lambda_0, \lambda_1, \lambda_2, \lambda_3,$ and λ_4, various fundamental solutions of Eq. (7) can be generated, leading to diverse wave structures such as solitons, periodic waves, and rational solutions.

Step (IV): Substitute the series expression from Eq. (6) and the auxiliary condition from Eq. (7) into Eq. (5). This yields a polynomial equation in terms of $\mathcal{W}(\zeta)$. By equating the coefficients of like powers of $\mathcal{W}(\zeta)$ to zero, a system of nonlinear algebraic equations is obtained. These equations can be systematically solved using symbolic computation software such as Wolfram Mathematica or Maple, enabling the determination of the unknown constants $\mathfrak{A}_i$, $\mathfrak{B}_i$, and λ_m. The resulting parameter sets provide a broad spectrum of exact analytical solutions for the original model given in Eq. (3).

2.2.1. Motivation for the improved modified extended Tanh-Function Method

The power of the IME tanh-function method is in its ability to produce a wider and physically valid set of exact solutions in contrast to other newly reported exact solutions in the recent past for the fractional nonlinear wave equations. While other methods, such as homotopy, perturbation, and transform methods, have been capable of providing only series solutions in a limited set of wave modes, the IME tanh method offers closed solutions in several forms of solution, such as dark, bright, singular, periodic, and Jacobi elliptic solutions, among others. Not only this, they do not have convergence and truncation errors, and also they do not require the usual mode limitations on the solutions compared to other methods reported in the recent past, and they also offer potential direct physical interpretations of the impact of the fractional parameters on the wave propagation phenomena, which is an added advantage. Further, as opposed to other reported methods in the recent past, this method also offers a bifurcation and comprehensive stability analysis in addition to solution construction, which is an added advantage and offers-in-depth physical understanding of the impact of parameters on the dynamics of such phenomena.

The applicability of each solution method depends on the structure of the model, including the type of PDE, boundary conditions, and the trade-off between computational efficiency and analytical tractability. While alternative approaches may provide broader generalization, the IME tanh-function method excels in producing precise and diverse solution structures, making it especially suitable for studying complex nonlinear phenomena such as soliton interactions, stability analysis, and bifurcation patterns.

3. Derivation of the model solutions

By applying the substitution $\mathcal{T} = \mathcal{Q}_x$ into Eq. (1), the equation transforms into the next NLPDE:

$$\left(D_t^{\beta}\mathcal{Q}_x + 6\mathcal{Q}_x\mathcal{Q}_{xx} + \mathcal{Q}_{xxxx}\right)_x - \varrho\mathcal{Q}_{xyy} + \mathcal{Q}_{xxxxy} + 3\mathcal{Q}_y\mathcal{Q}_{xxx} + 6\mathcal{Q}_{xx}\mathcal{Q}_{xy} + 3\mathcal{Q}_x\mathcal{Q}_{xxy} + D_t^{\beta}\mathcal{Q}_{xy} + \delta\mathcal{Q}_{xxy} = 0. \tag{8}$$

By implementing the transformation outlined in Eq. (4), Eq. (8) will transform to the next ODE:

$$2\mathcal{P}^{(5)} + 12\left(\mathcal{P}''\right)^2 + \left(\delta - 2\vartheta - \varrho + 12\mathcal{P}'\right)\mathcal{P}^{(3)} = 0. \tag{9}$$

By performing integration of Eq. (9) twice with respect to ζ, and neglecting the constants, the result is:

$$2\mathcal{P}^{(3)} + \mathcal{P}'\left(\delta - 2\vartheta - \varrho + 6\mathcal{P}'\right) = 0. \tag{10}$$

Let us consider $\mathcal{P}' = \Theta$, then Eq. (10) will be

$$2\Theta'' + 6\Theta^2 + (\delta - 2\vartheta - \varrho)\Theta = 0. \tag{11}$$

The principle of balance will be implemented to Eq.(11) among Θ^2 and Θ'', so $\mathbb{N} = 2$. Hence, one shall formulate the general form of the solution of Eq. (11) as:

$$\Theta(\xi) = \mathfrak{A}_0 + \mathfrak{A}_1\mathcal{W}(\xi) + \mathfrak{A}_2\mathcal{W}(\xi)^2 + \frac{\mathfrak{B}_1}{\mathcal{W}(\xi)} + \frac{\mathfrak{B}_2}{\mathcal{W}(\xi)^2}, \tag{12}$$

here $\mathfrak{A}_0, \mathfrak{A}_1, \mathfrak{A}_2, \mathfrak{B}_1$ and $\mathfrak{B}_2$ are constants that will be calculated, also $\mathfrak{A}_2$ and $, \mathfrak{B}_2 \neq 0$ together.

Equations (12) through (7) are inserted into Eq. (11), and the coefficients with similar powers equal zero. Thus, Mathematica software will be used to find the system's solutions. Thus, using the following examples, we were able to find the solutions of Eq. (2):

Case 1: $\lambda_0 = \lambda_1 = \lambda_3 = 0$,

(1.1) $\mathfrak{A}_0 = \mathfrak{A}_1 = \mathfrak{B}_1 = \mathfrak{B}_2 = 0,\ \mathfrak{A}_2 = -2\lambda_4,\ \varrho = \delta + 8\lambda_2 - 2\vartheta.$

(1.2) $\mathfrak{A}_0 = -\frac{4\lambda_2}{3},\ \mathfrak{A}_1 = \mathfrak{B}_1 = \mathfrak{B}_2 = 0,\ \mathfrak{A}_2 = -2\lambda_4,\ \varrho = \delta - 8\lambda_2 - 2\vartheta.$

In the context of case (1.1), the solutions of Eq.(2) can be categorized as follows:

(1.1.1) If $\lambda_2 > 0$ and $\lambda_4 < 0$, so a soliton solution of the bright type is gained as displayed next:

$$\mathcal{T}_{1.1.1} = 2\lambda_2\,\mathrm{sech}^2\left[\sqrt{\lambda_2}\left(x + y - \frac{\vartheta\left(t + \frac{1}{\Gamma(\beta)}\right)^{\beta}}{\beta}\right)\right]. \tag{13}$$

(1.1.2) If $\lambda_2 < 0$ and $\lambda_4 > 0$, so a periodic solution with singularity is displayed as described next:

$$\mathcal{T}_{1.1.2} = 2\lambda_2\,\sec^2\left[\sqrt{-\lambda_2}\left(x + y - \frac{\vartheta\left(t + \frac{1}{\Gamma(\beta)}\right)^{\beta}}{\beta}\right)\right]. \tag{14}$$

(1.1.3) If $\lambda_2 = 0$ and $\lambda_4 > 0$, a rational solution is displayed as described next:

$$\mathcal{T}_{1.1.3} = -\frac{2}{\left(x + y - \frac{\vartheta\left(t+\frac{1}{\Gamma(\beta)}\right)^{\beta}}{\beta}\right)^2}. \tag{15}$$

The solutions of Eq.(2) in case (1.2) fall into the following categories:
(1.2.1) If $\lambda_2 > 0$ and $\lambda_4 < 0$, a bright soliton solution is gained as displayed next:

$$\mathcal{T}_{1.2.1} = \frac{2\lambda_2}{3}\left(2 - 3\mathrm{sech}^2\left[\sqrt{\lambda_2}\left(x + y - \frac{\vartheta(t + \frac{1}{\Gamma(\beta)})^{\beta}}{\beta}\right)\right]\right). \tag{16}$$

(1.2.2) If $\lambda_2 < 0$ and $\lambda_4 > 0$, a singular periodic solution is displayed as described next:

$$\mathcal{T}_{1.2.2} = -\frac{2\lambda_2}{3}\left(2 - 3\sec^2\left[\sqrt{-\lambda_2}\left(x + y - \frac{\vartheta(t + \frac{1}{\Gamma(\beta)})^{\beta}}{\beta}\right)\right]\right). \tag{17}$$

(1.2.3) If $\lambda_2 = 0$ and $\lambda_4 > 0$, a rational solution is displayed as described next:

$$\mathcal{T}_{1.2.3} = -\frac{2}{3}\left(2\lambda_2 + \frac{3}{\left(x + y - \frac{\vartheta\left(t+\frac{1}{\Gamma(\beta)}\right)^{\beta}}{\beta}\right)^2}\right). \tag{18}$$

Case 2: $\lambda_1 = \lambda_3 = 0$, we get $\mathfrak{A}_1 = \mathfrak{B}_1 = 0$ and
(2.1) $\mathfrak{A}_0 = \frac{-2}{3}\left(\lambda_2 + \sqrt{\lambda_2^2 - 3\lambda_0\lambda_4}\right)$, $\mathfrak{A}_2 = 0$, $\mathfrak{B}_2 = -2\lambda_0$, $\varrho = \delta - 2\left(\vartheta + 4\sqrt{\lambda_2^2 - 3\lambda_0\lambda_4}\right)$.

(2.2) $\mathfrak{A}_0 = \frac{-2}{3}\left(\lambda_2 + \sqrt{\lambda_2^2 - 3\lambda_0\lambda_4}\right)$, $\mathfrak{A}_2 = -2\lambda_4$, $\mathfrak{B}_2 = 0$, $\varrho = \delta - 2\left(\vartheta + 4\sqrt{\lambda_2^2 - 3\lambda_0\lambda_4}\right)$.

(2.3) $\mathfrak{A}_0 = \frac{-2}{3}\left(\lambda_2 + \sqrt{\lambda_2^2 + 12\lambda_0\lambda_4}\right)$, $\mathfrak{A}_2 = -2\lambda_4$, $\mathfrak{B}_2 = -2\lambda_0$, $\varrho = \delta - 2\left(\vartheta + 4\sqrt{\lambda_2^2 + 12\lambda_0\lambda_4}\right)$.

The following categories can be used to group the solutions of Eq.(2) in case (2.1):
(2.1.1) If $\lambda_2 < 0$ and $\lambda_4 > 0$ and $\lambda_0 = \frac{\lambda_2^2}{4\lambda_4}$, singular soliton solution as described next:

$$\mathcal{T}_{2.1.1} = \lambda_2 \ \mathrm{csch}^2\left[\sqrt{-\lambda_2}\left(x + y - \frac{\vartheta\left(t + \frac{1}{\Gamma(\beta)}\right)^{\beta}}{\beta}\right)\right]. \tag{19}$$

(2.1.2) If $\lambda_2 > 0$, $\lambda_4 > 0$ and $\lambda_0 = \frac{\lambda_2^2}{4\lambda_4}$, a periodic solution with singularity as described next:

$$\mathcal{T}_{2.1.2} = -\lambda_2 \ \csc^2\left[\sqrt{\lambda_2}\left(x + y - \frac{\vartheta\left(t + \frac{1}{\Gamma(\beta)}\right)^{\beta}}{\beta}\right)\right]. \tag{20}$$

(2.1.3) If $\lambda_2>0,\ \lambda_4<0$ and $\lambda_0=\frac{\alpha^2\left(1-\alpha^2\right)\lambda_2^2}{\left(2\alpha^2-1\right)^2\lambda_4}$, a JEF solution is gained as displayed next:

$$\mathcal{T}_{2.1.3}=-\frac{2\lambda_2}{3\left(1-2\alpha^2\right)}\left(1-2\alpha^2+\sqrt{7\alpha^4-7\alpha^2+1}+3\left(1-\alpha^2\right)\mathrm{nc}^2\left[\sqrt{\frac{\lambda_2}{2\alpha^2-1}}\left(x+y-\frac{\vartheta\left(t+\frac{1}{\Gamma(\beta)}\right)^\beta}{\beta}\right)\right]\right), \tag{21}$$

where $0\leq\alpha\leq 1$.

A singular periodic solution is gained when we put $\alpha=0$ in Eq.(21) as described below:

$$\mathcal{T}_{2.1.3.a}=-\frac{2\lambda_2}{3}\left(2+3\sec^2\left[\sqrt{-\lambda_2}\left(x+y-\frac{\vartheta(t+\frac{1}{\Gamma(\beta)})^\beta}{\beta}\right)\right]\right). \tag{22}$$

(2.1.4) If $\lambda_2>0,\ \lambda_4<0$ and $\lambda_0=\frac{\left(1-\alpha^2\right)\lambda_2^2}{\left(2-\alpha^2\right)^2\lambda_4}$, a JEF is gained as displayed next:

$$\mathcal{T}_{2.1.4}=-\frac{2\lambda_2}{3\left(2-\alpha^2\right)}\left(2-\alpha^2-\sqrt{\alpha^4-\alpha^2+1}-\frac{3\left(1-\alpha^2\right)\lambda_2}{\alpha^2}\mathrm{nd}^2\left[\sqrt{\frac{\lambda_2}{2-\alpha^2}}\left(x+y-\frac{\vartheta\left(t+\frac{1}{\Gamma(\beta)}\right)^\beta}{\beta}\right)\right]\right). \tag{23}$$

(2.1.5) If $\lambda_2>0,\ \lambda_4<0$ and $\lambda_0=\frac{\alpha^2\lambda_2^2}{\left(\alpha^2+1\right)^2\lambda_4}$, a JEF is gained as displayed next:

$$\mathcal{T}_{2.1.5}=-\frac{2\lambda_2}{3\left(\alpha^2+1\right)}\left(1+\alpha^2+\sqrt{\alpha^4-\alpha^2+1}-3\mathrm{ns}^2\left[\sqrt{-\frac{\lambda_2}{\alpha^2+1}}\left(x+y-\frac{\vartheta\left(t+\frac{1}{\Gamma(\beta)}\right)^\beta}{\beta}\right)\right]\right). \tag{24}$$

A singular soliton solution is gained when we put $\alpha=1$ in Eq.(24) as described below:

$$\mathcal{T}_{2.1.5.a}=\lambda_2\ \mathrm{csch}^2\left[\left(x+y-\frac{\vartheta(t+\frac{1}{\Gamma(\beta)})^\beta}{\beta}\right)\sqrt{\frac{-\lambda_2}{2}}\right]. \tag{25}$$

A singular periodic solution is gained when we put $\alpha=0$ in Eq.(24) as described below:

$$\mathcal{T}_{2.1.5.b}=-\frac{2\lambda_2}{3}\left(2-3\csc^2\left[\sqrt{-\lambda_2}\left(x+y-\frac{\vartheta(t+\frac{1}{\Gamma(\beta)})^\beta}{\beta}\right)\right]\right). \tag{26}$$

The solutions to Eq.(2) in case (2.2) fall into the following categories:

(2.2.1) If $\lambda_2<0$ and $\lambda_4>0$ and $\lambda_0=\frac{\lambda_2^2}{4\lambda_4}$, a bright soliton solution is gained as displayed next:

$$\mathcal{T}_{2.2.1}=-\lambda_2\ \mathrm{sech}^2\left[\sqrt{-\lambda_2}\left(x+y-\frac{\vartheta\left(t+\frac{1}{\Gamma(\beta)}\right)^\beta}{\beta}\right)\right]. \tag{27}$$

(2.2.2) If $\lambda_2>0,\ \lambda_4>0$ and $\lambda_0=\frac{\lambda_2^2}{4\lambda_4}$, then one can get the following solution, which is called singular periodic:

$$\mathcal{T}_{2.2.2}=\lambda_2\ \sec^2\left[\left(x+y-\frac{\vartheta(t+\frac{1}{\Gamma(\beta)})^\beta}{\beta}\right)\sqrt{\frac{\lambda_2}{2}}\right]. \tag{28}$$

(2.2.3) If $\lambda_2 > 0,\ \lambda_4 < 0$ and $\lambda_0 = \frac{\alpha^2\left(1-\alpha^2\right)\lambda_2^2}{\left(2\alpha^2-1\right)^2\lambda_4}$, a JEF solution is gained as displayed next:

$$\mathcal{T}_{2.2.3} = -\frac{2\lambda_2}{3\left(1-2\alpha^2\right)}\left(1-2\alpha^2+\sqrt{7\alpha^4-7\alpha^2+1}+3\alpha^2\mathrm{cn}^2\left[\sqrt{\frac{\lambda_2}{2\alpha^2-1}}\left(x+y-\frac{\vartheta\left(t+\frac{1}{\Gamma(\beta)}\right)^\beta}{\beta}\right)\right]\right). \tag{29}$$

(2.2.4) If $\lambda_2 > 0,\ \lambda_4 < 0$ and $\lambda_0 = \frac{\left(1-\alpha^2\right)\lambda_2^2}{\left(2-\alpha^2\right)^2\lambda_4}$, a JEF is gained as displayed next:

$$\mathcal{T}_{2.2.4} = -\frac{2\lambda_2}{3\left(2-\alpha^2\right)}\left(2-\alpha^2-\sqrt{\alpha^4-\alpha^2+1}+\frac{3\alpha^2}{\lambda_2}\mathrm{dn}^2\left[\sqrt{\frac{\lambda_2}{2-\alpha^2}}\left(x+y-\frac{\vartheta\left(t+\frac{1}{\Gamma(\beta)}\right)^\beta}{\beta}\right)\right]\right). \tag{30}$$

(2.2.5) If $\lambda_2 > 0,\ \lambda_4 < 0$ and $\lambda_0 = \frac{\alpha^2\lambda_2^2}{\left(\alpha^2+1\right)^2\lambda_4}$, a JEF is gained as displayed next:

$$\mathcal{T}_{2.2.5} = -\frac{2\lambda_2}{3\left(\alpha^2+1\right)}\left(1+\alpha^2+\sqrt{\alpha^4-\alpha^2+1}-3\alpha^2\mathrm{ns}^2\left[\sqrt{-\frac{\lambda_2}{\alpha^2+1}}\left(x+y-\frac{\vartheta\left(t+\frac{1}{\Gamma(\beta)}\right)^\beta}{\beta}\right)\right]\right). \tag{31}$$

A bright soliton solution is gained when we put $\alpha = 1$ in Eq.(31) as described below:

$$\mathcal{T}_{2.2.5.a} = -\lambda_2\ \mathrm{sech}^2\left[\left(x+y-\frac{\vartheta(t+\frac{1}{\Gamma(\beta)})^\beta}{\beta}\right)\sqrt{\frac{-\lambda_2}{2}}\right]. \tag{32}$$

The solutions of Eq.(2) in case (2.3) fall into the following categories:

(2.3.1) If $\lambda_2 < 0$ and $\lambda_4 > 0$ and $\lambda_0 = \frac{\lambda_2^2}{4\lambda_4}$, then one can get the following solution, which is called a singular soliton:

$$\mathcal{T}_{2.3.1} = -4\lambda_2\ \mathrm{csch}^2\left[\sqrt{-2\lambda_2}\left(x+y-\frac{\vartheta\left(t+\frac{1}{\Gamma(\beta)}\right)^\beta}{\beta}\right)\right]. \tag{33}$$

(2.3.2) If $\lambda_2 > 0,\ \lambda_4 > 0$ and $\lambda_0 = \frac{\lambda_2^2}{4\lambda_4}$, a singular periodic solution is gained as displayed next:

$$\mathcal{T}_{2.3.2} = -4\lambda_2\ \csc^2\left[\sqrt{2\lambda_2}\left(x+y-\frac{\vartheta\left(t+\frac{1}{\Gamma(\beta)}\right)^\beta}{\beta}\right)\right]. \tag{34}$$

(2.3.3) If $\lambda_2 > 0,\ \lambda_4 < 0$ and $\lambda_0 = \frac{\alpha^2\left(1-\alpha^2\right)\lambda_2^2}{\left(2\alpha^2-1\right)^2\lambda_4}$, a JEF solution is gained as displayed next:

$$\mathcal{T}_{2.3.3} = -\frac{2\lambda_2}{3\left(1-2\alpha^2\right)}\left(1-2\alpha^2+\sqrt{8\alpha^4-8\alpha^2+1}+3\alpha^2\mathrm{cn}^2\left[\zeta\sqrt{\frac{\lambda_2}{2\alpha^2-1}}\right]+3\left(1-\alpha^2\right)\mathrm{nc}^2\left[\zeta\sqrt{\frac{\lambda_2}{2\alpha^2-1}}\right]\right), \tag{35}$$

where $\zeta = x + y - \frac{\vartheta\left(t+\frac{1}{\Gamma(\beta)}\right)^{\beta}}{\beta}$.

(2.3.4) If $\lambda_2 > 0$, $\lambda_4 < 0$ and $\lambda_0 = \frac{(1-\alpha^2)\lambda_2^2}{(2-\alpha^2)^2\lambda_4}$, a JEF is gained as displayed next:

$$\mathcal{T}_{2.3.4} = -\frac{2\lambda_2}{3\left(2-\alpha^2\right)}\left(2-\alpha^2-\sqrt{\alpha^4-16\alpha^2+16}+\frac{3\alpha^2}{\lambda_2}\mathrm{dn}^2\left[\zeta\sqrt{\frac{\lambda_2}{2-\alpha^2}})\right]+\frac{3\left(1-\alpha^2\right)\lambda_2}{\alpha^2}\mathrm{nd}^2\left[\zeta\sqrt{\frac{\lambda_2}{2-\alpha^2}}\right]\right), \tag{36}$$

where $\zeta = x + y - \frac{\vartheta\left(t+\frac{1}{\Gamma(\beta)}\right)^{\beta}}{\beta}$.

(2.3.5) If $\lambda_2 > 0$, $\lambda_4 < 0$ and $\lambda_0 = \frac{\alpha^2\lambda_2^2}{(\alpha^2+1)^2\lambda_4}$, a JEF is gained as displayed next:

$$\mathcal{T}_{2.3.5} = -\frac{2\lambda_2}{3\left(\alpha^2+1\right)}\left(1+\alpha^2+\sqrt{\alpha^4+14\alpha^2+1}-3\alpha^2\mathrm{ns}^2\left[\zeta\sqrt{-\frac{\lambda_2}{\alpha^2+1}}\right]-3\mathrm{sn}^2\left[\zeta\sqrt{-\frac{\lambda_2}{\alpha^2+1}}\right]\right), \tag{37}$$

where $\zeta = x + y - \frac{\vartheta\left(t+\frac{1}{\Gamma(\beta)}\right)^{\beta}}{\beta}$.

A bright soliton solution is gained when we put $\alpha = 1$ in Eq.(37) as described below:

$$\mathcal{T}_{2.3.5.a} = -\lambda_2\ \mathrm{sech}^2\left[\left(x+y-\frac{\vartheta(t+\frac{1}{\Gamma(\beta)})^{\beta}}{\beta}\right)\sqrt{\frac{\lambda_2}{2}}\right]. \tag{38}$$

<u>Case 3:</u> If $\lambda_2 = \lambda_4 = 0$, we get

$\mathfrak{A}_0 = \frac{(\sqrt{21}+3)\lambda_1^2}{24\lambda_0}$, $\mathfrak{A}_1 = 0$, $\mathfrak{B}_1 = -\lambda_1$, $\mathfrak{A}_2 = 0$, $\mathfrak{B}_2 = -2\lambda_0$, $\varrho = \delta + \frac{\sqrt{21}\lambda_1^2}{2\lambda_0} - 2\vartheta$, $\lambda_3 = -\frac{\lambda_1^3}{8\lambda_0^2}$.

This finding will result in the following Weierstrass elliptic function form for the solution of Eq. (2):

$$\mathcal{T}_3 = \frac{\left(\sqrt{21}+3\right)\lambda_1^2}{24\lambda_0} - \frac{\lambda_1}{\wp\left[\zeta\sqrt{-\frac{\lambda_1^3}{32\lambda_0^2}};\frac{32\lambda_0^2}{\lambda_1^2},\frac{32\lambda_0^3}{\lambda_1^3}\right]} - \frac{2\lambda_0}{\wp\left[\zeta\sqrt{-\frac{\lambda_1^3}{32\lambda_0^2}};\frac{32\lambda_0^2}{\lambda_1^2},\frac{32\lambda_0^3}{\lambda_1^3}\right]^2}. \tag{39}$$

<u>Case 4:</u> If $\lambda_3 = \lambda_4 = 0$, we get

(4.1) $\mathfrak{A}_0 = \mathfrak{A}_1 = \mathfrak{A}_2 = 0$, $\mathfrak{B}_1 = -2\sqrt{\lambda_0\lambda_2}$, $\mathfrak{B}_2 = -2\lambda_0$, $\varrho = \delta+2\lambda_2-2\vartheta$, $\lambda_1 = 2\sqrt{\lambda_0\lambda_2}$.

(4.2) $\mathfrak{A}_0 = -\frac{\lambda_2}{3}$, $\mathfrak{A}_1 = \mathfrak{A}_2 = 0$, $\mathfrak{B}_1 = -2\sqrt{\lambda_0\lambda_2}$, $\mathfrak{B}_2 = -2\lambda_0$, $\varrho = \delta - 2\lambda_2 - 2\vartheta$, $\lambda_1 = 2\sqrt{\lambda_0\lambda_2}$.

(4.3) $\mathfrak{A}_0 = \mathfrak{A}_1 = \mathfrak{B}_1 = \mathfrak{A}_2 = \lambda_1 = 0$, $\mathfrak{B}_2 = -2\lambda_0$, $\varrho = \delta + 8\lambda_2 - 2\vartheta$.

(4.4) $\mathfrak{A}_0 = -\frac{4\lambda_2}{3}$, $\mathfrak{A}_1 = \mathfrak{B}_1 = \mathfrak{A}_2 = \lambda_1 = 0$, $\mathfrak{B}_2 = -2\lambda_0$, $\varrho = \delta - 8\lambda_2 - 2\vartheta$.

Within the results of case (4.1), the solution of Eq.(2) will be in exponential form as follows:

$$\mathcal{T}_{4.1} = -\frac{2\sqrt{\lambda_0\lambda_2^3}\; e^{\sqrt{\lambda_2}\left(x+y-\frac{\vartheta\left(t+\frac{1}{\Gamma(\beta)}\right)^{\beta}}{\beta}\right)}}{\left(\sqrt{\lambda_0}-\sqrt{\lambda_2}e^{\sqrt{\lambda_2}\left(x+y-\frac{\vartheta\left(t+\frac{1}{\Gamma(\beta)}\right)^{\beta}}{\beta}\right)}\right)^2}, \tag{40}$$

where $\lambda_2 > 0$ and $\lambda_0 = \frac{\lambda_1^2}{4\lambda_2}$.
According to the outcomes of set (4.1), the solution of Eq. (2) will have the following exponential form:

$$\mathcal{T}_{4.2} = -\frac{\lambda_2}{3} - \frac{2\sqrt{\lambda_0\lambda_2^3}e^{\sqrt{\lambda_2}\left(x+y-\frac{\vartheta\left(t+\frac{1}{\Gamma(\beta)}\right)^{\beta}}{\beta}\right)}}{\left(\sqrt{\lambda_0}-\sqrt{\lambda_2}e^{\sqrt{\lambda_2}\left(x+y-\frac{\vartheta\left(t+\frac{1}{\Gamma(\beta)}\right)^{\beta}}{\beta}\right)}\right)^2}, \tag{41}$$

where $\lambda_2 > 0$ and $\lambda_0 = \frac{\lambda_1^2}{4\lambda_2}$.
The solutions of Eq.(2) in case (4.3) fall into the following categories:
(4.3.1) If $\lambda_1 = 0,\ \lambda_0 > 0$ and $\lambda_2 < 0,$ then one can get the following solution, which is called singular periodic:

$$\mathcal{T}_{4.3.1} = 2\lambda_2 \mathrm{csc}^2\left[\left(x+y-\frac{\vartheta\left(t+\frac{1}{\Gamma(\beta)}\right)^{\beta}}{\beta}\right)\sqrt{-\lambda_2}\right]. \tag{42}$$

(4.3.2) If $\lambda_1 = 0,\ \lambda_0 > 0$ and $\lambda_2 > 0,$ then one can get the following solution, which is called a singular soliton:

$$\mathcal{T}_{4.3.2} = -2\lambda_2 \mathrm{csch}^2\left[\left(x+y-\frac{\vartheta\left(t+\frac{1}{\Gamma(\beta)}\right)^{\beta}}{\beta}\right)\sqrt{\lambda_2}\right]. \tag{43}$$

The solutions of Eq.(2) in case (4.4) fall into the following categories:

(4.4.1) If $\lambda_1 = 0,\ \lambda_0 > 0$ and $\lambda_2 < 0,$ then one can get the following solution, which is called singular periodic:

$$\mathcal{T}_{4.4.1} = -\frac{4\lambda_2}{3} + 2\lambda_2 \mathrm{csc}^2\left[\left(x+y-\frac{\vartheta\left(t+\frac{1}{\Gamma(\beta)}\right)^{\beta}}{\beta}\right)\sqrt{-\lambda_2}\right]. \tag{44}$$

(4.4.2) If $\lambda_1 = 0,\ \lambda_0 > 0$ and $\lambda_2 > 0,$ then one can get the following solution, which is called a singular soliton:

$$\mathcal{T}_{4.4.2} = -\frac{4\lambda_2}{3} - 2\lambda_2 \text{csch}^2\left[\left(x + y - \frac{\vartheta\left(t + \frac{1}{\Gamma(\beta)}\right)^{\beta}}{\beta}\right)\sqrt{\lambda_2}\right]. \tag{45}$$

Case 5: If $\lambda_0 = \lambda_1 = 0$, we get
(5.1) $\mathfrak{A}_0 = \mathfrak{A}_1 = \mathfrak{B}_1 = \mathfrak{B}_2 = \lambda_3 = 0,\ \mathfrak{A}_2 = -2\lambda_4,\ \varrho = \delta + 8\lambda_2 - 2\vartheta.$
(5.2) $\mathfrak{A}_0 = -\frac{4\lambda_2}{3},\ \mathfrak{A}_1 = \mathfrak{B}_1 = \mathfrak{B}_2 = \lambda_3 = 0,\ \mathfrak{A}_2 = -2\lambda_4,\ \varrho = \delta - 8\lambda_2 - 2\vartheta.$
(5.3) $\mathfrak{A}_0 = \mathfrak{B}_1 = \mathfrak{B}_2 = 0,\ \mathfrak{A}_1 = -2\sqrt{\lambda_2\lambda_4},\ \mathfrak{A}_2 = -2\lambda_4,\ \varrho = \delta + 2\lambda_2 - 2\vartheta,\ \lambda_3 = 2\sqrt{\lambda_2\lambda_4}.$
(5.4) $\mathfrak{A}_0 = -\frac{\lambda_2}{3},\ \mathfrak{A}_1 = -2\sqrt{\lambda_2\lambda_4},\ \mathfrak{B}_1 = \mathfrak{B}_2 = 0,\ \mathfrak{A}_2 = -2\lambda_4,\ \varrho = \delta - 2\lambda_2 - 2\vartheta,\ \lambda_3 = 2\sqrt{\lambda_2\lambda_4}.$

The solutions of Eq.(2) in case (5.1) fall into the following categories:

(5.1.1) If $\lambda_2 < 0$ and $\lambda_3 \neq 2\sqrt{\lambda_2\lambda_4}$, a singular periodic solution is displayed as described next:

$$\mathcal{T}_{5.1.1} = 2\lambda_2 \csc^2\left[\left(x + y - \frac{\vartheta\left(t + \frac{1}{\Gamma(\beta)}\right)^{\beta}}{\beta}\right)\sqrt{-\lambda_2}\right]. \tag{46}$$

(5.1.2) If $\lambda_2 > 0$ and $\lambda_3 \neq 2\sqrt{\lambda_2\lambda_4}$, a singular soliton solution is displayed as described next:

$$\mathcal{T}_{5.1.2} = -2\lambda_2 \text{csch}^2\left[\left(x + y - \frac{\vartheta\left(t + \frac{1}{\Gamma(\beta)}\right)^{\beta}}{\beta}\right)\sqrt{\lambda_2}\right]. \tag{47}$$

The solutions of Eq.(2) in case (5.2) fall into the following categories:

(5.2.1) If $\lambda_2 < 0$ and $\lambda_3 \neq 2\sqrt{\lambda_2\lambda_4},$ then one can get the following solution, which is called singular periodic:

$$\mathcal{T}_{5.2.1} = -\frac{2\lambda_2}{3}\left(2 - 3\csc^2\left[\left(x + y - \frac{\vartheta\left(t + \frac{1}{\Gamma(\beta)}\right)^{\beta}}{\beta}\right)\sqrt{-\lambda_2}\right]\right). \tag{48}$$

(5.2.2) If $\lambda_2 > 0$ and $\lambda_3 \neq 2\sqrt{\lambda_2\lambda_4}$, a singular soliton solution is displayed as described next:

$$\mathcal{T}_{5.2.2} = -\frac{2\lambda_2}{3}\left(2 + 3\text{csch}^2\left[\left(x + y - \frac{\vartheta\left(t + \frac{1}{\Gamma(\beta)}\right)^{\beta}}{\beta}\right)\sqrt{\lambda_2}\right]\right). \tag{49}$$

A solution of Eq. (2) in the case (5.3) results in a dark soliton form as follows:

$$\mathcal{T}_{5.3} = -\lambda_2 \left(\frac{3}{2} + 2\tanh\left[\zeta \frac{\sqrt{\lambda_2}}{2}\right] + +\frac{1}{2}\tanh^2\left[\zeta \frac{\sqrt{\lambda_2}}{2}\right] \right), \tag{50}$$

such that $\zeta = \left(x + y - \frac{\vartheta\left(t+\frac{1}{\Gamma(\beta)}\right)^{\beta}}{\beta} \right)$ and $\lambda_2 < 0$ and $\lambda_3 = 2\sqrt{\lambda_2\lambda_4}$.

A solution of Eq. (2) in the case (5.4) results in a dark soliton form as follows:

$$\mathcal{T}_{5.4.1} = -\lambda_2 \left(\frac{11}{6} + 2\tanh\left[\zeta \frac{\sqrt{\lambda_2}}{2}\right] + +\frac{1}{2}\tanh^2\left[\zeta \frac{\sqrt{\lambda_2}}{2}\right] \right), \tag{51}$$

where $\zeta = \left(x + y - \frac{\vartheta\left(t+\frac{1}{\Gamma(\beta)}\right)^{\beta}}{\beta} \right)$, $\lambda_2 < 0$ and $\lambda_3 = 2\sqrt{\lambda_2\lambda_4}$.

4. Graphical and physical representations of some extracted solutions

This section presents numerical simulations with three distinct values of β to illustrate the physical representations of various solutions using 2D, 3D, contour, and polar charts. The selected solutions are visualized through 3D, contour, polar, and 2D plots using carefully chosen model parameter values. Under the assumptions that $\vartheta = 0.6,\ \lambda_2 = 1.6,\ y = 0$, and $0 \le x \le 8$, Figure (1) depicts the solution aligned with Eq. (13), which is a bright soliton in 3-D, contour, 2-D, and polar forms. These visualizations confirm the existence of stable bright solitons within the model and directly illustrate how fundamental physical characteristics of such solitons (intensity, shape, and spatial scale) are tunable via the fractional derivative order β. This provides critical insight into possible applications in wave guiding and signal processing in fractional media. Assuming $\vartheta = 0.5,\ \lambda_2 = -0.65,\ y = 0$, and $0 \le x \le 8$, Figure (2) explains the singular periodic solution aligned with Eq. (14) in 3-D, contour, 2-D, and polar forms. Such plots have distinct features like various occurrences of singularity. Moreover, periodicity in wave characteristics can be seen in these figures across the spatial domain. Changes in the fractional parameter β have an obvious impact on the sharpness and intensity of the singularity. Furthermore, periodicity is distinctly evident in the polar plot characteristics. In 3-D, contour, 2-D, and polar forms, Figure (3) displays the solution aligned with Eq. (19), which is a singular soliton under the assumptions that $\vartheta = 0.7,\ \lambda_2 = -1.7,\ y = 0$, and $0 \le x \le 15$. Under the assumptions that $\vartheta = 0.75,\ \lambda_2 = 1.75,\ y = 0$, and $0 \le x \le 15$. These plots illustrate sharp localized singularity behaviors whose strength and location are further modified by the variation of β. Contour plots and polar plots further demonstrate how singularity solutions' geometry and symmetry are changed for different values of β. The importance of considering symmetry in singular wave solutions is evident. Figure (4) displays the dark soliton solution aligned with Eq. (50) in 3-D, contour, 2-D, and polar forms. Dark solitons are localized, stagnant regions or troughs of reduced intensity traveling through an otherwise constant, uniform background. They describe waves with intensive non-linearity, which are commonplace in non-linear optics, Bose–Einstein condensates, plasma waves, etc. As the value of β increases, so does the degree of sharpness of this notch or trough, which implies that stronger fractional material possesses stronger confining abilities for dark excitations.

5. Transformation into a Planar Dynamical System

Let us consider the nonlinear differential equation of the second order

$$6\mathcal{T}^2 + (\delta - 2\vartheta - \varrho)\mathcal{T} + 2\mathcal{T}'' = 0,$$

in which the quantities $\delta, \vartheta, \varrho \in \mathbb{R}$ are real constants. To simplify notation, introduce the parameter

$$\eta := \delta - 2\vartheta - \varrho,$$

which transforms the equation into the compact form

$$6\mathcal{T}^2 + \eta\mathcal{T} + 2\mathcal{T}'' = 0. \tag{52}$$

Since it is often more convenient to analyze planar autonomous systems rather than higher-order equations, we recast Eq. (52) as a system of first-order differential equations. Define new state variables

$$x = \mathcal{T}, \qquad y = \mathcal{T}'.$$

Consequently,

$$x' = y, \qquad y' = \mathcal{T}''.$$

Substituting these relations into (52) yields

$$6x^2 + \eta x + 2y' = 0,$$

or equivalently

$$y' = -3x^2 - \frac{\eta}{2}x.$$

Thus, the original problem is reduced to the following equivalent planar system

$$\begin{cases} x' = y, \\ y' = -3x^2 - \frac{\eta}{2}x. \end{cases}$$

This reformulation allows us to study the qualitative behavior of solutions by employing tools from dynamical systems theory, such as phase-plane analysis, equilibrium classification, and bifurcation theory. In what follows, we examine stability properties and explore how changes in the parameter η modify the phase portrait.

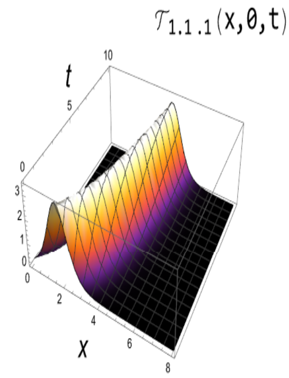

(a) 3D Plot ($\beta = 0.3$)

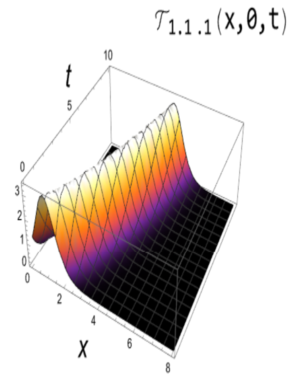

(b) 3D Plot ($\beta = 0.6$)

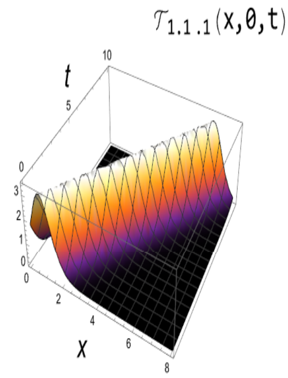

(c) 3D Plot ($\beta = 1.0$)

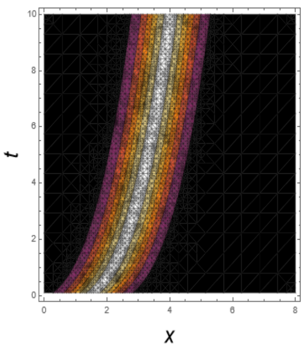

(d) Contour Plot ($\beta = 0.3$)

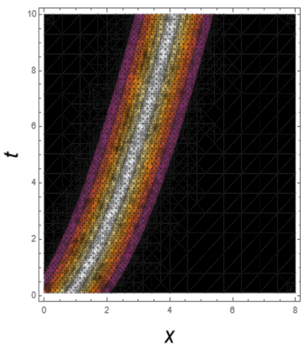

(e) Contour Plot ($\beta = 0.6$)

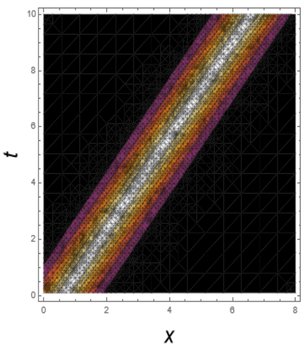

(f) Contour Plot ($\beta = 1.0$)

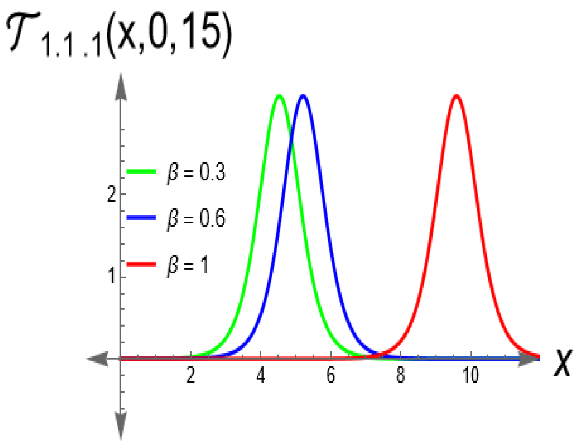

(g) 2D plot with different β

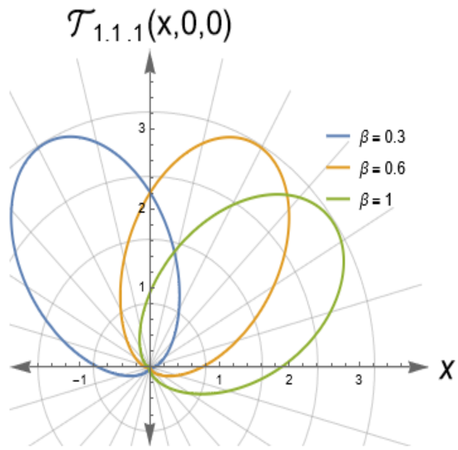

(h) Ploar plot with different β

Figure 1: 3D, contour, 2D and polar plots for the bright soliton solution introduced by Eq. (13).

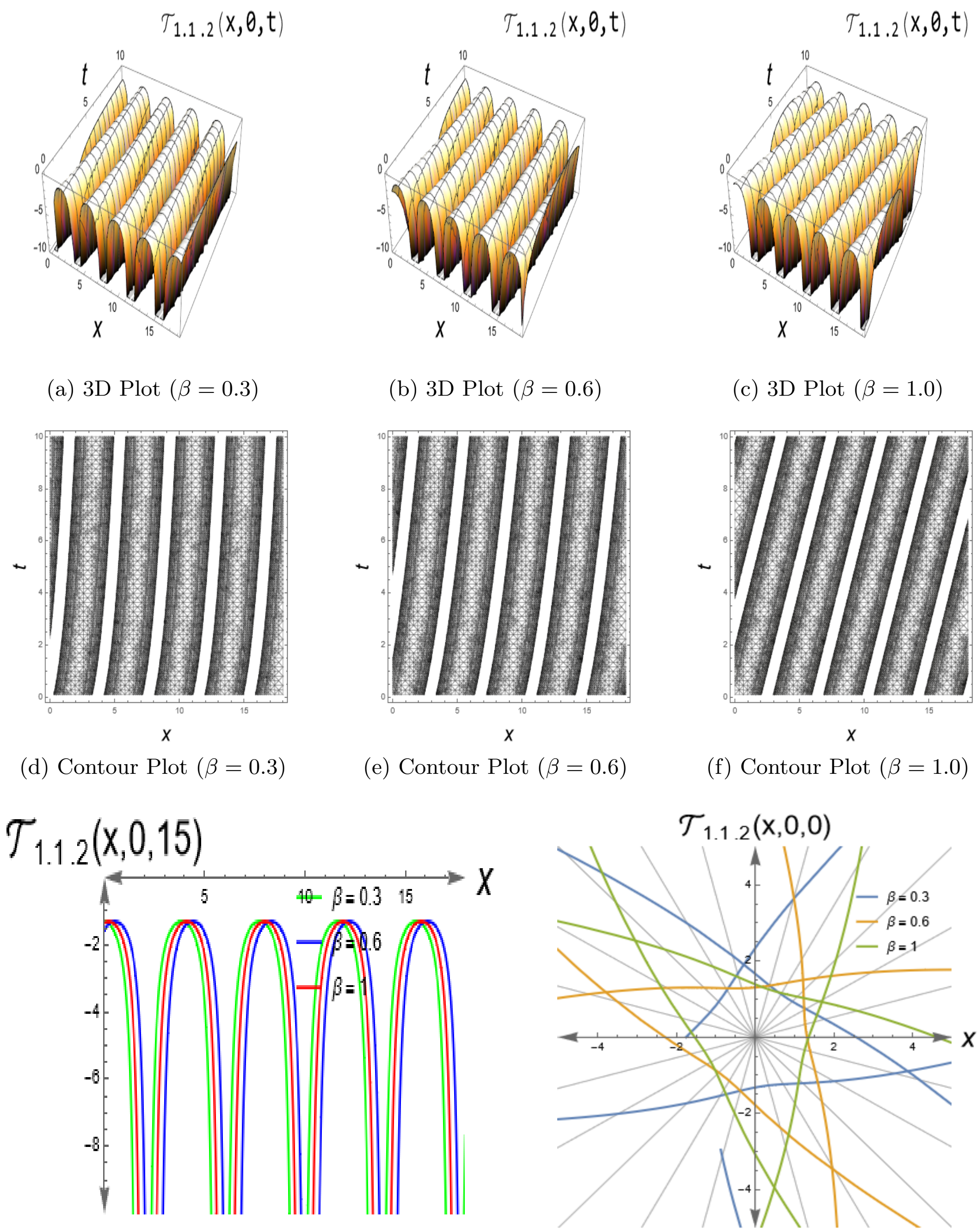

(a) 3D Plot ($\beta = 0.3$) (b) 3D Plot ($\beta = 0.6$) (c) 3D Plot ($\beta = 1.0$)

(d) Contour Plot ($\beta = 0.3$) (e) Contour Plot ($\beta = 0.6$) (f) Contour Plot ($\beta = 1.0$)

(g) 2D plot with different β (h) Polar plot with different β

Figure 2: 3D, contour, 2D and polar plots for the singular periodic solution introduced by Eq. (14).

6. Stability and Bifurcation Properties

We now focus attention on the autonomous system

$$\begin{cases} x' = y, \\ y' = 3x^2 + \eta x, \end{cases} \tag{53}$$

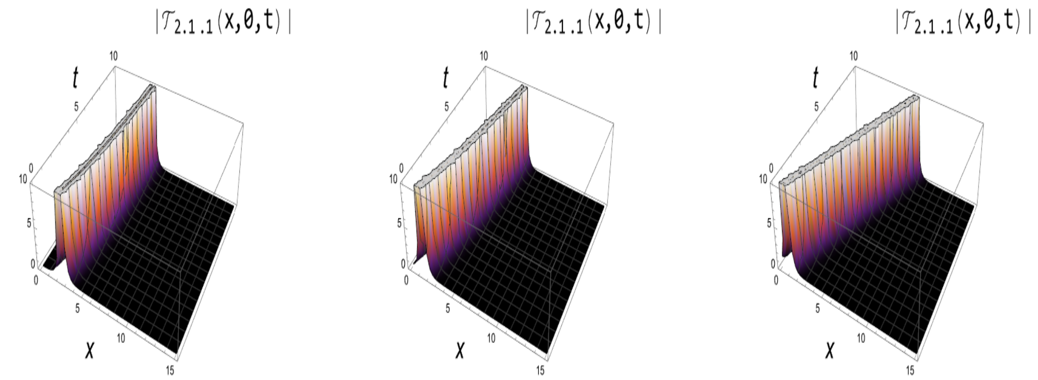

(a) 3D Plot ($\beta = 0.3$) (b) 3D Plot ($\beta = 0.6$) (c) 3D Plot ($\beta = 1.0$)

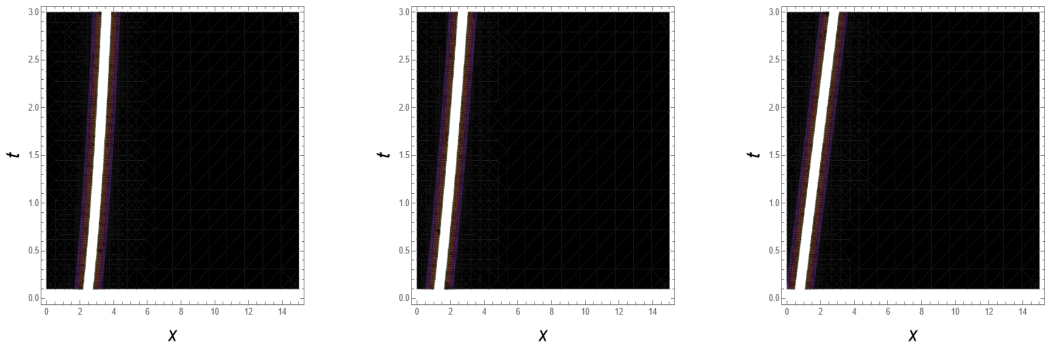

(d) Contour Plot ($\beta = 0.3$) (e) Contour Plot ($\beta = 0.6$) (f) Contour Plot ($\beta = 1.0$)

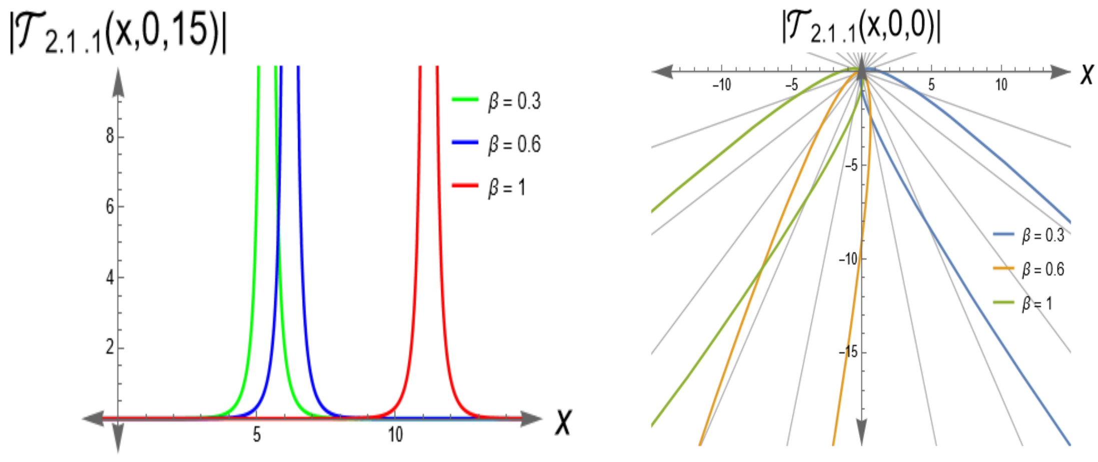

(g) 2D plot with different β (h) Polar plot with different β

Figure 3: 3D, contour, 2D and polar plots for the singular soliton solution introduced by Eq. (19).

where $\eta \in \mathbb{R}$ acts as a bifurcation parameter governing the system's dynamics.

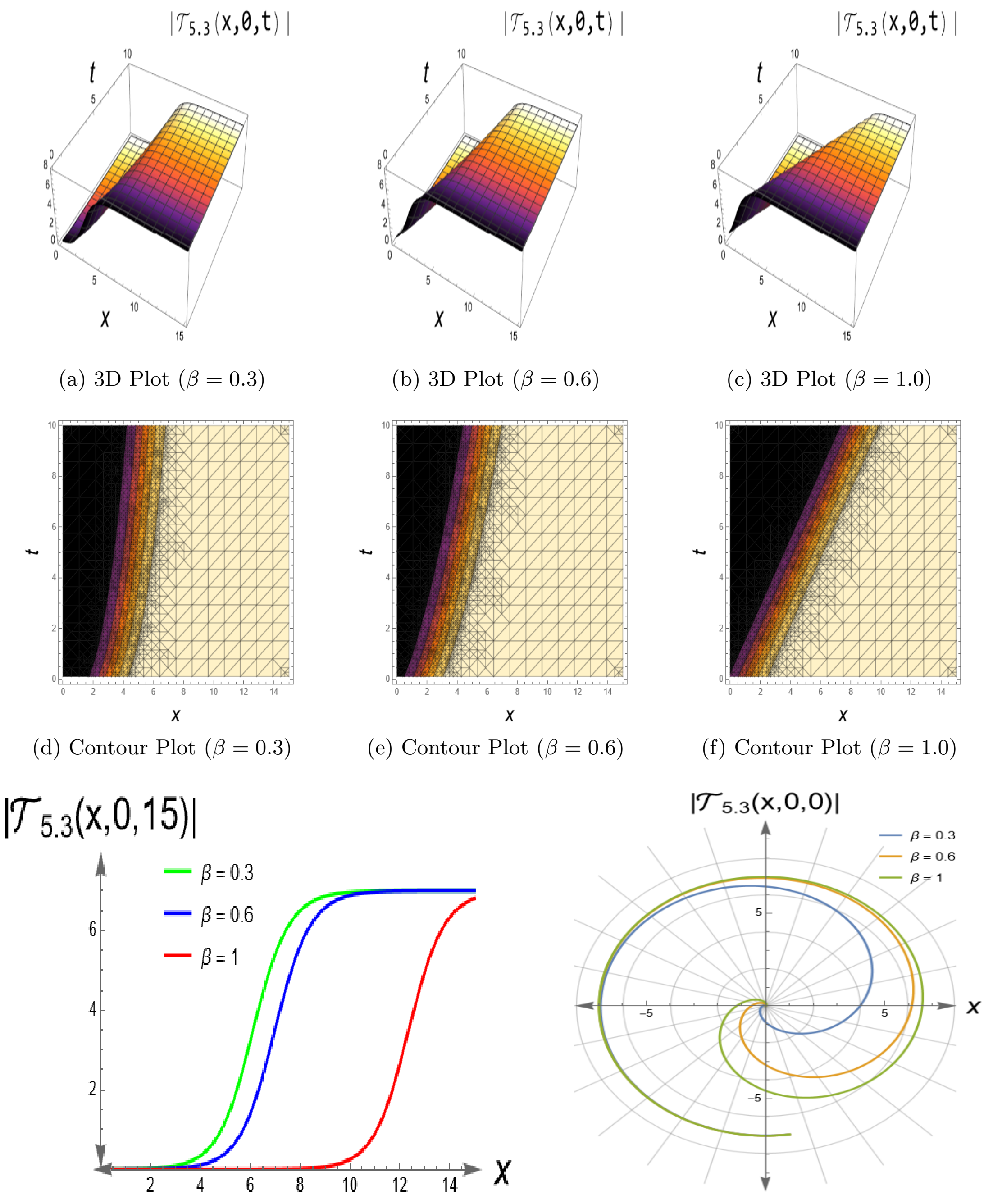

(a) 3D Plot ($\beta = 0.3$) (b) 3D Plot ($\beta = 0.6$) (c) 3D Plot ($\beta = 1.0$)

(d) Contour Plot ($\beta = 0.3$) (e) Contour Plot ($\beta = 0.6$) (f) Contour Plot ($\beta = 1.0$)

(g) 2D plot with different β (h) Polar plot with different β

Figure 4: 3D, contour, 2D and polar plots for the dark soliton solution introduced by Eq. (50).

Equilibria

The stationary points of (53) are determined by solving

$$x' = 0, \quad y' = 0.$$

From $x' = y = 0$ and $3x^2 + \eta x = 0$, we obtain

$$x(3x + \eta) = 0,$$

which leads to the two equilibria

$$E_1 = (0, 0), \qquad E_2 = \Big(-\tfrac{\eta}{3}, 0 \Big).$$

Linearization and Local Stability

To assess the nature of these equilibria, we linearize the system. The Jacobian matrix at a general point (x, y) is

$$J(x, y) = \begin{bmatrix} 0 & 1 \\ 6x + \eta & 0 \end{bmatrix}.$$

At $E_1 = (0, 0)$: We have

$$J(0, 0) = \begin{bmatrix} 0 & 1 \\ \eta & 0 \end{bmatrix}.$$

The characteristic polynomial is

$$\mu^2 - \eta = 0 \quad \Longrightarrow \quad \mu = \pm\sqrt{\eta}.$$

Hence:

- For $\eta > 0$, the eigenvalues are real with opposite signs, so the origin is a saddle point (unstable).
- For $\eta = 0$, both eigenvalues vanish, yielding a degenerate equilibrium.
- For $\eta < 0$, the eigenvalues are purely imaginary, corresponding to a linear center.

At $E_2 = (-\frac{\eta}{3}, 0)$: Substituting into the Jacobian gives

$$J\Big(-\tfrac{\eta}{3}, 0 \Big) = \begin{bmatrix} 0 & 1 \\ -\eta & 0 \end{bmatrix}.$$

The characteristic equation becomes

$$\mu^2 + \eta = 0 \quad \Longrightarrow \quad \mu = \pm\sqrt{-\eta}.$$

Thus:

- For $\eta < 0$, the equilibrium is a saddle point.
- For $\eta = 0$, the eigenvalues are zero, giving degeneracy.
- For $\eta > 0$, the eigenvalues are purely imaginary, and the point behaves like a center.

Bifurcation Scenario

The system (53) undergoes a transition as the parameter η varies through zero:

- When $\eta < 0$: the origin is a center, while $E_2 = \left(-\frac{\eta}{3}, 0\right)$ is a saddle point.
- When $\eta = 0$: both equilibria collide at the origin, structuring a degenerate equilibrium.
- When $\eta > 0$: the origin becomes a saddle, and the shifted equilibrium turns into a center.

An iconic illustration of a **saddle–center bifurcation** is this parameter-driven role reversal between the two fixed points. A saddle and a center reside on opposing sides of the bifurcation threshold, trade stability, and unite at the crucial parameter value in such a bifurcation.

Phase portraits showing the qualitative dynamics of system (53) for specific values of the parameter η are represented in Figure (5), highlighting the transition associated with a saddle–center bifurcation.

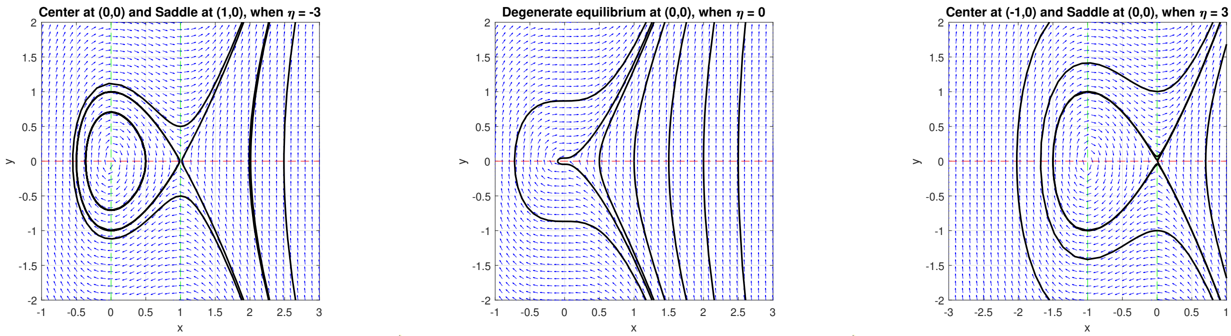

(a) (b) (c)

Figure 5: Phase portraits illustrating the qualitative behavior of system (53) for representative values of the parameter η. The transition reflects the occurrence of a saddle–center bifurcation.

7. Physical Interpretation and Model Validation

The derived analytical solutions of the (2+1)-dimensional Kadomtsev-Petviashvili equation with the beta-fractional derivative offer valuable physical understanding of the nonlinear wave motion in complex dispersive media. The appearance of dark, bright, singular, periodic, and elliptic wave solutions corresponds to various physical scenarios of localized wave structures, wave depression, and periodic patterns that may occur in plasma physics, shallow water waves, and nonlinear optics. The beta-fractional derivative is essential in determining the amplitude, width, and wave speed of these waves, which can be shown in all 2D plots in figures (1-g), (2-g), (3-g), and (4-g).

To ensure the physical validity of the analytical solutions, stability and bifurcation analyses were performed to determine the parameter ranges where stable and physically valid wave solutions exist. The graphical simulations also support the analytical results by demonstrating the evolution and interaction properties of the solitons for different fractional parameters. These findings demonstrate the capability of the proposed model in describing the nonlinear wave dynamics in fractional media and provide a firm foundation for future numerical and experimental studies to validate its applicability in real-world physical systems.

8. Conclusions

In this manuscript, the IME tanh function method is used to explore the dynamical behavior of the (2+1)-dimensional Kadomtsev–Petviashvili model with the effect of the beta-fractional derivative. This work was performed for the first time on this specific formulation. It yielded many exact analytical solutions, including dark, bright, and singular solitons, exponential solutions, Weierstrass elliptic solutions, JEFs, and singular periodic wave solutions. Additionally, demonstrating how these solutions are affected by the beta-fractional derivative. Additionally, this publication incorporates stability and bifurcation analysis to provide a detailed investigation of the discovered solutions. Several graphical visualizations were provided in order to illustrate the dynamic aspects and physical interpretations of the resulting solutions. Future research could focus on investigating the stability analysis, numerical simulations, and possible applications in nonlinear wave propagation in complex media in order to expand on the current analysis of the $(2+1)$-dimensional Kadomtsev–Petviashvili model with the effect of the beta-fractional derivative. Including variable-order fractional derivatives or external perturbation variables might potentially provide further light on the model's dynamic behavior and physical importance. Furthermore, on the basis of these studies, future research will use numerical simulations to properly validate the stability of the results derived through analytical methods under different physical perturbations. For further refining the realistic nature of the model, future research can be conducted to include stochastic terms such as multiplicative noise terms to properly study models of waves propagating through noisy, random media, or as an alternate method, techniques such as the homotopy analysis method or Adomian's decomposition method can be applied to extend the results to include variable-order fractional models, to name one such scenario.

Acknowledgements

The project was funded by KAU Endowment (WAQF) at King Abdulaziz University, Jeddah, Saudi Arabia. The authors, therefore, acknowledge with thanks WAQF and the Deanship of Scientific Research (DSR) for technical and financial support.

References

[1] A. S. Khalifa, H. M. Ahmed, N. M. Badra, and W. B. Rabie. Exploring solitons in optical twin-core couplers with Kerr law of nonlinear refractive index using the modified extended direct algebraic method. *Optical and Quantum Electronics*, 56(6):1060, 2024.

[2] P. Albayrak. Optical solitons of Biswas–Milovic model having spatio-temporal dispersion and parabolic law via a couple of Kudryashov's schemes. *Optik*, 279:170761, 2023.

[3] W. X. Ma. Lump solutions to the Kadomtsev–Petviashvili equation. *Physics Letters A*, 379(36):1975–1978, 2015.

[4] K. K. Ahmed, N. M. Badra, H. M. Ahmed, and W. B. Rabie. Soliton solutions and other solutions for Kundu–Eckhaus equation with quintic nonlinearity and Raman effect using the improved modified extended tanh function method. *Mathematics*, 10:1–11, 2022.

[5] Z. Li and S. Zhao. Bifurcation, chaotic behavior and solitary wave solutions for the Akbota equation. *AIMS Mathematics*, 9:22590–22601, 2024.

[6] R. Hao, L. Li, Z. Li, W. Xue, and G. Zhou. A new approach to exact soliton solutions and soliton interaction for the nonlinear Schrödinger equation with variable coefficients. *Optics Communications*, 236:79–86, 2004.

[7] M. Bilal, Shafqat-Ur-Rehman, and J. Ahmad. Dispersive solitary wave solutions for the dynamical soliton model by three versatile analytical mathematical methods. *The European Physical Journal Plus*, 137(6):674, 2022.

[8] M. Bilal and J. Ahmad. A variety of exact optical soliton solutions to the generalized (2+ 1)-dimensional dynamical conformable fractional Schrödinger model. *Results in Physics*, 33:105198, 2022.

[9] J. Ahmad. Dispersive multiple lump solutions and soliton's interaction to the nonlinear dynamical model and its stability analysis. *The European Physical Journal D*, 76(1):14, 2022.

[10] Shafqat-Ur-Rehman, M. Bilal, and J. Ahmad. New exact solitary wave solutions for the 3D-FWBBM model in arising shallow water waves by two analytical methods. *Results in Physics*, 25:104230, 2021.

[11] S. Ahmad, S. Saifullah, A. Khan, and M. Inc. New local and nonlocal soliton solutions of a nonlocal reverse space–time mKdV equation using improved Hirota bilinear method. *Physics Letters A*, 450:128393, 2022.

[12] T. Y. Zhou, B. Tian, C. R. Zhang, and S. H. Liu. Auto-Bäcklund transformations, bilinear forms, multiple-soliton, quasi-soliton and hybrid solutions of a (3+1)-dimensional modified Korteweg–de Vries-Zakharov-Kuznetsov equation in an electron-positron plasma. *European Physical Journal Plus*, 137:912, 2022.

[13] X. H. Wu, Y. T. Gao, X. Yu, C. C. Ding, and L. Q. Li. Modified generalized Darboux transformation and solitons for a Lakshmanan-Porsezian-Daniel equation. *Chaos, Solitons & Fractals*, 162:112399, 2022.

[14] W. X. Ma, Y. Huang, and F. Wang. Inverse scattering transforms and soliton solutions of nonlocal reverse-space nonlinear Schrödinger hierarchies. *Studies in*

Applied Mathematics, 145:563–585, 2020.

[15] M. S. Ghayad, N. M. Badra, H. M. Ahmed, W. B. Rabie, H. Rezazadeh, and M. A. Hosseinzadeh. Extraction of new optical solitons of conformable time fractional generalized RKL equation via quadrupled power-law of self-phase modulation. *Optical and Quantum Electronics*, 56(8):1304, 2024.

[16] A. S. Khalifa, N. M. Badra, H. M. Ahmed, and W. B. Rabie. Retrieval of optical solitons in fiber Bragg gratings for high-order coupled system with arbitrary refractive index. *Optik*, 287:171116, 2023.

[17] K. K. Ahmed, N. M. Badra, H. M. Ahmed, W. B. Rabie, M. Mirzazadeh, M. Eslami, and M. S. Hashemi. Investigation of solitons in magneto-optic waveguides with Kudryashov's law nonlinear refractive index for coupled system of generalized nonlinear Schrödinger's equations using modified extended mapping method. *Nonlinear Analysis: Modelling and Control*, 29(2):205–223, 2024.

[18] K. J. Wang. An effective computational approach to the local fractional low-pass electrical transmission lines model. *Alexandria Engineering Journal*, 110:629–635, 2025.

[19] K. J. Wang and S. Li. Study on the local fractional (3+ 1)-dimensional modified Zakharov–Kuznetsov equation by a simple approach. *Fractals*, 32(05):2450091, 2024.

[20] K. J. Wang, F. Shi, and J. H. Liu. Soliton molecules and the novel hybrid interaction solutions of the new extended (3+ 1)-dimensional Boiti–Leon–Manna–Pempinelli equation. *Pramana*, 98(2):67, 2024.

[21] K. J. Wang. The generalized (3+ 1)-dimensional B-type Kadomtsev–Petviashvili equation: resonant multiple soliton, N-soliton, soliton molecules and the interaction solutions. *Nonlinear Dynamics*, 112(9):7309–7324, 2024.

[22] M. Kaplan, A. Bekir, and A. Akbulut. A generalized Kudryashov method to some nonlinear evolution equations in mathematical physics. *Nonlinear Dynamics*, 85:2843–2850, 2016.

[23] D. Chou, H. Ur Rehman, A. Amer, and A. Amer. New solitary wave solutions of generalized fractional Tzitzéica-type evolution equations using Sardar sub-equation method. *Optical and Quantum Electronics*, 55:1148, 2023.

[24] M. I. Khan, S. Asghar, and J. Sabi'u. Jacobi Elliptic function expansion method for the improved modified Korteweg-de Vries equation. *Optical and Quantum Electronics*, 54:734, 2022.

[25] N. K. Vitanov, Z. I. Dimitrova, and K. N. Vitanov. On the use of composite functions in the Simple Equations Method to obtain exact solutions of nonlinear differential equations. *Computation*, 9:104, 2021.

[26] K. K. Ahmed, N. M. Badra, H. M. Ahmed, and W. B. Rabie. Soliton solutions and other solutions for Kundu–Eckhaus equation with quintic nonlinearity and Raman effect using the improved modified extended tanh function method. *Mathematics*, 10:4203, 2022.

[27] K. K. Ahmed, N. M. Badra, H. M. Ahmed, and W. B. Rabie. Soliton solutions of generalized Kundu-Eckhaus equation with an extra-dispersion via improved modi-

fied extended tanh function technique. *Optical and Quantum Electronics*, 55(299):1–17, 2023.

[28] M. U. Shahzad, H. U. Rehman, A. U. Awan, Z. Zafar, A. M. Hassan, and I. Iqbal. Analysis of the exact solutions of nonlinear coupled Drinfeld–Sokolov–Wilson equation through ϕ^6-model expansion method. *Results in Physics*, 52:106771, 2023.

[29] M. S. Ghayad, N. M. Badra, H. M. Ahmed, and W. B. Rabie. Derivation of optical solitons and other solutions for nonlinear Schrödinger equation using a modified extended direct algebraic method. *Alexandria Engineering Journal*, 64:801–811, 2023.

[30] W. B. Rabie, K. K. Ahmed, N. M. Badra, H. M. Ahmed, M. Mirzazadeh, and M. Eslami. New solitons and other exact wave solutions for coupled system of perturbed highly dispersive CGLE in birefringent fibers with polynomial nonlinearity law. *Optical and Quantum Electronics*, 56(5):1–22, 2024.

[31] S. T. R. Rizvi, A. R. Seadawy, A. Bashir, and Nimra. Lie symmetry analysis and conservation laws with soliton solutions to a nonlinear model related to chains of atoms. *Optical and Quantum Electronics*, 55:762, 2023.

[32] S. Luo, W. Li, X. Li, and Q. Wei. Stochastic representation for solutions of a system of coupled HJB-Isaacs equations with integral–differential operators. *Stochastic Processes and their Applications*, 179:104502, 2025.

[33] Y. Rostami. New technique for solving system of variable-order fractional partial integro differential equations. *Computational Mathematics and Mathematical Physics*, 65(2):270–289, 2025.

[34] S. J. Chen, X. Lü, and Y. H. Yin. Dynamic behaviors of the lump solutions and mixed solutions to a (2+1)-dimensional nonlinear model. *Communications in Theoretical Physics*, 75(5):055005, 2023.

[35] M. Madadi and M. Inc. Dynamics of localized waves and interactions in a (2+1)-dimensional equation from combined bilinear forms of Kadomtsev–Petviashvili and extended shallow water wave equations. *Wave Motion*, 134:103455, 2025.

[36] S. J. Chen, X. Lü, and Y. H. Yin. Dynamic behaviors of the lump solutions and mixed solutions to a (2+ 1)-dimensional nonlinear model. *Communications in Theoretical Physics*, 75(5):055005, 2023.

[37] A. Altalbe, A. A. Zaagan, A. Bekir, and A. Cevikel. The nonlinear wave dynamics of the space-time fractional van der Waals equation via three analytical methods. *Physics of Fluids*, 36:027140, 2024.

[38] M. Gu, J. Li, F. Liu, Z. Li, and C. Peng. Propagation of traveling wave solution of the strain wave equation in microcrystalline materials. *Open Physics*, 2024.

[39] S. Zhao. Chaos analysis and traveling wave solutions for fractional (3+1)-dimensional Wazwaz Kaur Boussinesq equation with beta derivative. *Scientific Reports*, 14:23034, 2024.

[40] A. C. Cevikel, A. Bekir, and Ö. Guner. Exploration of new solitons solutions for the Fitzhugh–Nagumo-type equations with conformable derivatives. *International Journal of Modern Physics B*, 37:2350224, 2023.

[41] Abdon Atangana and Rubayyi T Alqahtani. Modelling the spread of river blind-

ness disease via the Caputo fractional derivative and the beta-derivative. *Entropy*, 18(2):40, 2016.

[42] Mahmoud Soliman, Hamdy M Ahmed, Niveen M Badra, Islam Samir, Taha Radwan, and Karim K Ahmed. Fractional wave structures in a higher-order nonlinear Schrödinger equation with cubic–quintic nonlinearity and β-fractional dispersion. *Fractal and Fractional*, 9(8):522, 2025.

[43] I. Podlubny. *Fractional differential equations: an introduction to fractional derivatives, fractional differential equations, to methods of their solution and some of their applications*, volume 198. Elsevier, 1998.

[44] D. Baleanu, T. Kalmar-Nagy, T. P. Sapsis, and H. Yabuno. Nonlinear Dynamics: Models, Behavior, and Techniques. *Journal of Computational and Nonlinear Dynamics*, 13(9):090301, 2018.